Islamic Azad University

Journal of

Optoelectronical Nanostructures

Summer 2019 / Vol. 4, No. 3

Propose, Analysis and Simulation of an All Optical Full Adder Based on Plasmonic Waves using Metal-Insulator-Metal Waveguide Structure

Mohsen Olyaee[*,1], Mohammad Bagher Tavakoli[1], Abbas Mokhtari[1]

[1] Department of Electronic Engineering, Arak Branch, Islamic Azad University, Arak, Iran

(Received 10 Jun. 2019; Revised 21 Jul. 2019; Accepted 8 Aug. 2019; Published 15 Sep. 2019)

Abstract: This paper proposes a full adder with minimum power consumption and low loss with a central frequency of 1550nm using plasmonic Metal-Insulator-Metal (MIM) waveguide structure and rectangular cavity resonator. This full adder operates based on XOR and AND logic gates. In this full adder, the resonant wave composition of the first and second modes has been used and we have obtained a high transmission coefficient in the states in which the output must be active. This full adder uses the AND and XOR logic gates to be designed with three inputs, which results in the design of a full adder with lower complexity, lower cost and fewer losses than Other full adders in which AND and XOR logic gates are combined to be designed with two inputs. The related simulations were performed by FDTD. The obtained results presented a performance similar to the predicted models, while considering approximations with theoretical relations.

Keywords: Cavity Resonator, MIM Waveguide, full-adder

1. INTRODUCTION

Optical control is one of the main issues in all-optical integrated circuits [1]. These circuits are widely used in all-optical communication networks. Optical computations have been used since 1980s [1-2]. However, the research trend on this issue has decreased due to limitations of materials used, avoiding optical-chip miniaturization, and cost reduction in laboratory research. The main reason behind this trend has been optical diffraction in optical devices which can be solved using plasmonic waves [1]. The introduction of plasmonic structures as well as technological approaches toward optical electronic circuit integration alongside development issues and phenomena that may prevent further compaction have led scientists to analyse plasmonic structures and plasmonic waves. Because of increased centralized optical field intensity in very small

* Corresponding author. Email: **moaer@iautb.ac.ir**

sizes and sub-waveform, surface plasmons can be used as an appropriate substrate for development of all-optical devices. Owing to the conductivity of surface plasmons in dielectric-metal cross part, MIM waveguides are special among plasmonic devices, since waveguides not only support emissions with very small wavelengths and higher group velocity, but also illustrate wave conductibility for relatively higher distances [4]. The combination of these waveguides and nano-resonators with various side coupled forms leads to novel different structures with widespread applications across all-optical devices [1, 2]. Optical fibre is the transfer medium in optical networks, where the wavelength band used for data transfer is in the third window, 1550nm, with a minimum power loss. Thus, a full-adder has been designed for the wavelength of 1550 nm (1530-1565 C-Band) [4,6]. This paper is organized as follows. Section 1 provides an overview of the research conducted on the topic of releasing of plasmonic waves. In Section 2, we describe the equations of the theory of plasmonic structures and define the basis for the design of the full adder. Then, the mathematical equations of the electrical permeability coefficient are expressed in a plasmonic structure and wave equation, and also the constant propagation of the plasmonic waves from the dispersion relation is obtained. In this section, we further provide relations for the various modes of magnetic fields in the plasmonic waveguide, and obtain the intensity of the magnetic field in the first mode, which is very important. In Sections 4 and 5, the logic gates AND and XOR are proposed to perform simulations for the design of all-optical full adder. In Section 6, using the logic gates designed in Sections 4 and 5, an all-optical half-adder is proposed, and the results of the simulation output are presented. Finally, in Section 7, we first design and then simulate the logic gate AND and XOR of the new plasmonic with three inputs. Thereafter, using these two gates, we will propose the all-optical full adder based on the plasmonic wave at the central frequency of 1550 nm.

Plasmonics are defined as an interaction between electromagnetic waves and conduction electrons in nano-sized metals. Plasmonic waveguides and many optical devices have been proposed in recent research based on the emission of surface plasmons [3, 4]. In [3], all-optical logic gates with plasmonic waveguide have been introduced/simulated using Y-shaped waveguide divider Figs. However, the problem of the theory has not been addressed in this section. Also, the optical power drop in this structure is noticeable. In an all-optical ICs, there is a need for several logic gates connected in series. If each gate has a huge power loss, practical implementation will not be feasible. In [4], a photonic crystal waveguide and nonlinear features of optical materials have been employed for designing all-optical logic gates. Although nonlinear photonic crystal structures have various important applications, they suffer from several shortcomings in logic gates compared to plasmonic structures, including increased piece size and higher power loss. In [5], full-absorption in periodic

plasmonic nanoparticles and optical power pump in these nanoparticles have been utilized in order to change the output and create AND logic gate. Although this is a novel design, it has higher development complexity for a simple logic gate and the piece size is large and power consumption is higher due to constant optical power pumping. In [6], the author has proposed basic logic gates using plasmonic waveguides and slot cavity resonator whichuses the transfer coefficient of wave amplitudes in waveguides. Thus, considering that the number of input ports varies across different modes, the amplitude transfer coefficient cannot practically illustrate the changes in the output (when a wave radiates into one of the inputs, the transfer coefficient at the output will be the ratio of wave amplitude at the output to the wave amplitude at the input port.If the wave radiates into both input ports, the transfer coefficient at the output will be the ratio of wave amplitude at the output to the combined value of both waves at the input).Further, all computations of structure design will be difficult and the author should consider wave amplitude at the output port as the measure of operation[7-10]. In this paper, the plasmonic structure and slot cavity resonator have been utilized for designing a full adder. In this regard, first, AND and XOR logic gates [11-18,20] required for designing an adder are proposed and then numerical simulations are completed using FDTD.

2. THEORETICAL RELATIONSHIPS of PLASMONIC STRUCTURES

In this paper, a nanometer-sized MIM waveguide between two metal structures is used for implementing the logic gates. Fig. 1 depicts the proposed typical schema of this structure in this paper.

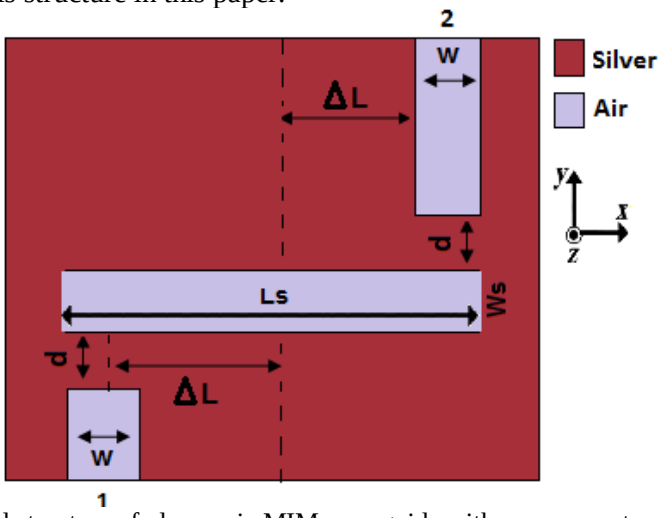

Fig.1. Typical structure of plasmonic MIM waveguide with nanoresonator rectangular cavity

When the distance between two metals is very small, surface plasmons may be excited, with plasmonic waves emitted between two metals used as a messenger. In this paper, air is considered as the insulator and silver constitutes the metals used as in Drude model. The relative dielectric function for metals in Drude model is expressed by Eq. [8]:

$$\varepsilon_m(\omega) = \varepsilon_\infty - \frac{\omega_p^2}{\omega(\omega + j\gamma)} \quad (1)$$

Where,ε_∞ is the dielectric coefficient of the material with infinite frequency, $\omega_p$represents the plasma frequency, and γ denotes the damping angular frequency. The value of the separameters for silver are: $\omega_p = 9.1\, e.v\,, \gamma = .018\, e.v$, and $\varepsilon_\infty = 3.7$. The width of waveguides is taken as 100 nm in order to stimulate only the first and second modes (TM0, TM1). Also, either the first mode or second mode can be used given the device application. By solving Maxwell relationships, one can obtain dispersion relation in Eq. (2).

$$\tanh\left(\frac{k_d}{2}w\right) = -\frac{\varepsilon_d\, k_m}{\varepsilon_m k_d} \quad (2)$$

Where,ε_d is the insulator dielectric coefficient (i.e., the air that is unity), ε_m represents the metal dielectric coefficient (silver).k_d and $k_m$denote the wave numbers related to the dielectric and metal, respectively.

If the complex emission constant in plasmonic waveguide is β, one can obtain Eqs. (3) and (4) simply by embedding electrical and magnetic fields within the dielectric and metal using boundary conditions.

$$k_d = \sqrt{(\beta^2 - \varepsilon_d k_0^2)} \quad (3)$$

$$k_m = \sqrt{(\beta^2 - \varepsilon_m k_0^2)} \quad (4)$$

By solving Eqs. (2)-(4) simultaneously, the emission constant in the waveguide (β) can be obtained.

Consider Fig. 1 that is the basic illustration of these studies, consisting of a MIM waveguide and a rectangular cavity with a length of Ls. Once the MIM waveguide is excited and resonance conditions are established in a rectangular cavity, plasmonic waves will be stationary with consecutive sweeps. The resonance occurs when a phase shift developed byconsecutive sweeps in the cavity (along with phase differences which are developed at the ends of the cavity) is an integer proportion of π, that is $\Delta\varphi = \beta_m L_s + \varphi_r = m\pi$. This can be neglected considering negligibility of φ_r.

If the refractive index in plasmonic waveguides and resonance cavity is n_{eff} where $k_0 = 2\pi/\lambda$ is the wavenumber in vacuum, then $n_{eff} = \beta/k_0$ is obtained as follows:

$$\beta_m L_s = m\pi \Longrightarrow n_{eff}.\frac{2\pi}{\lambda_m}.L_s = m\pi \Longrightarrow \lambda_m = \frac{2L_s.n_{eff}}{m} \quad (5)$$

If the input port in Fig. 1 is excited by an electromagnetic wave at optical frequencies, electrical and magnetic fields in stationary resonance in the rectangular cavity can be obtained by solving Maxwell equations. The intensity of magnetic fields in the resonator nanogap for *m*th mode is obtained using Eq. (6).

$$H_m(x,t) = \frac{2H_0\cos(\beta_m x - \frac{\beta_m.L_S}{2})}{\sigma}\left[e^{j\left(\frac{3}{2}\beta_m.L_m - \beta_m.\Delta L\right)} + e^{j\left(\beta_m.\Delta L - \frac{1}{2}\beta_m.L_m\right)}\right] \quad (6)$$

In Eq. (6), ΔL is the distance between the input port and rectangular nanoslot. Typically, waveguides reach the edge of nanogap. Thus, $\Delta L = \frac{L_S}{2}$ (definitely, it can be less than this value with no compromise). Considering that the width of waveguides is very small, only the first and second modes are excited in nanoslots. For example, the relationship of the first-mode magnetic field is given by Eq. (7).

$$m = 1 \Longrightarrow H_m(x,t) = \frac{2H_0.\sin(\beta_1.x)}{\sigma}\left[-\sin(\beta_1.\Delta L)e^{-j(\omega_1.t)}\right] \quad (7)$$

Eq. (7) is used to gain an idea to inform the design of XOR, OR, and AND logics which are the required legs of an adder. If two input waveguides are considered with a skew-symmetric distance from the nanoresonator center , i.e., one is ΔL_1 and another is $\Delta L_2 = -\Delta L_1$, two resonated magnetic fields will neutralize each other in the rectangular cavity, leading to zero field inside this cavity. In addition, the output parameters of interest may be acquired with the increase in the number of waveguides and their distance can be adjusted.

3. XOR LOGIC GATE

For designing XOR logic gate which is required for all full-adders, Fig. 2 can be considered.

The inputs 1 and 2 are the same as the bits a, b; if the amplitude of the electrical field of the radiated optical wave is 1, it means logic ‘1’’; otherwise logic ‘0’. The output port indicates that the result bit is XOR logic gate; however, if the electrical field intensity in the output port is greater than 0.4, this will be logic ‘1’; while, if it is less than 0.4, it will be logic ‘0’.

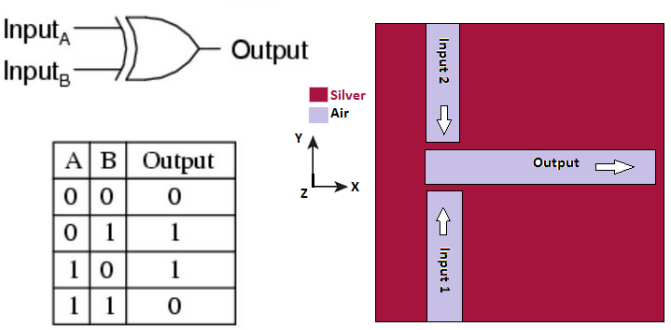

A	B	Output
0	0	0
0	1	1
1	0	1
1	1	0

Fig.2. Designed XOR structure; red indicates *silver* while blue indicates *air*. Width of waveguides and nanoresonators is 100nm, the length is 555 nm, the distance between nanoresonators and waveguides is 10 nm, and the depth of silver is 50 nm.

In Fig. 3a, the lower input port is uniformly excited by electromagnetic waves with amplitude of 1. In this case, as demonstrated in Fig. 3b, the plasmonic waves will be resonated and excited at a wavelength of 1550nm and a small area around it (the plasmonic waveguide band). Fig. 3c displays the magnitude of the electric field on the output port, which is about 0.62 units, indicating high transmission coefficient (equal to 0.62) and low losses of this logical optical gate. Note that in Fig. 3b, the size of the passing factor was observed to be about 0.31 at 1550nm, which is different from the obtained number of field divisions in the output port in relation to the field domain at the input port (0.62). This is because the Lumerical software does not have a correct resolution due to the two input ports, and calculates the transmittance coefficient of the two input ports finally representing the transmittance coefficient as half of the real value. In these structures, the best way to calculate the field amplitude in the output port is to calculate the transmission coefficient, while the simulator transfer coefficient diagram is only appropriate for calculating the resonance centre frequency and bandwidth. Fig. 3d reveals the amplitude of the fields in the equipment and the input/output ports.

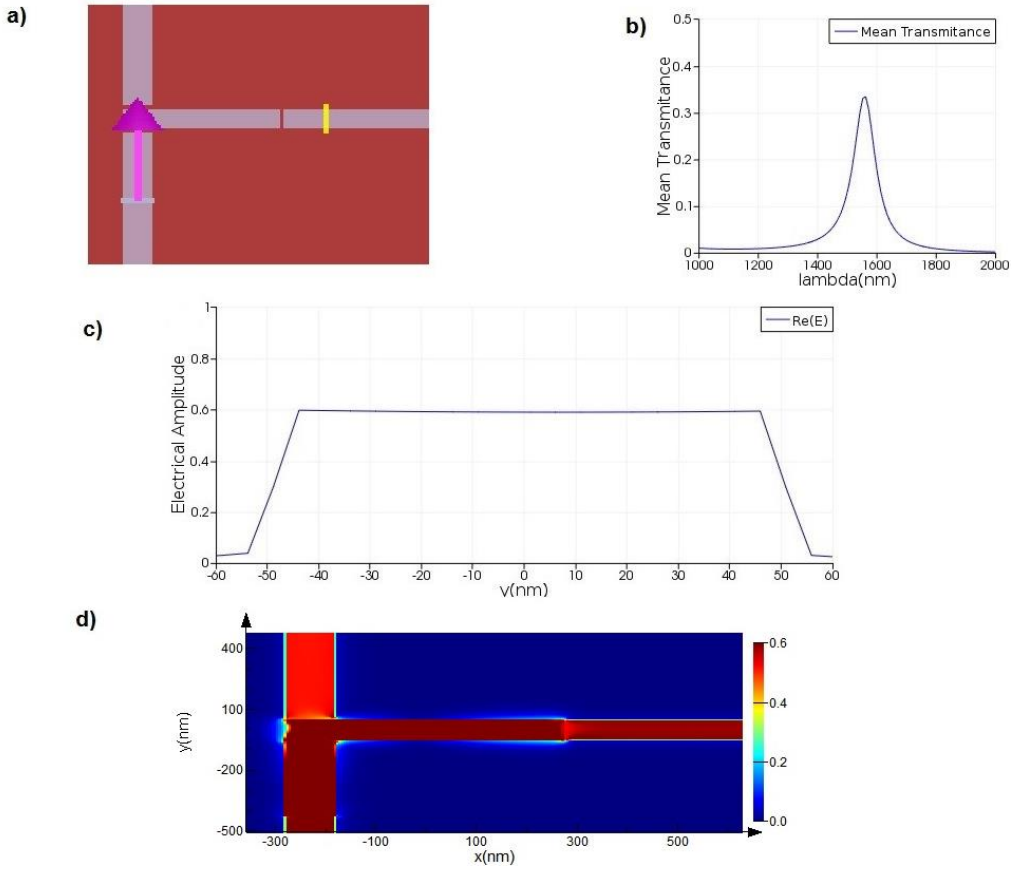

Fig.3. The structure of xor is designed, a) the stimulation mode with the lower input port, b) the resonance curve in the rectangular nanosorator, c) the electric field amplitude at 1550nm at the output port, d) the display of the fields in the gate structure at wavelengths 1550nm.

In Fig. 4a, we stimulate two input ports with a single-bandwidth domain. In this case, the amplitude of the electric field of the output port is observed at 1550nm in Fig. 4b. As can be seen, the range of the field is zero suggesting the proper performance of the XOR gate. Fig. 4c displays the range of fields in the equipment and the input/output ports.

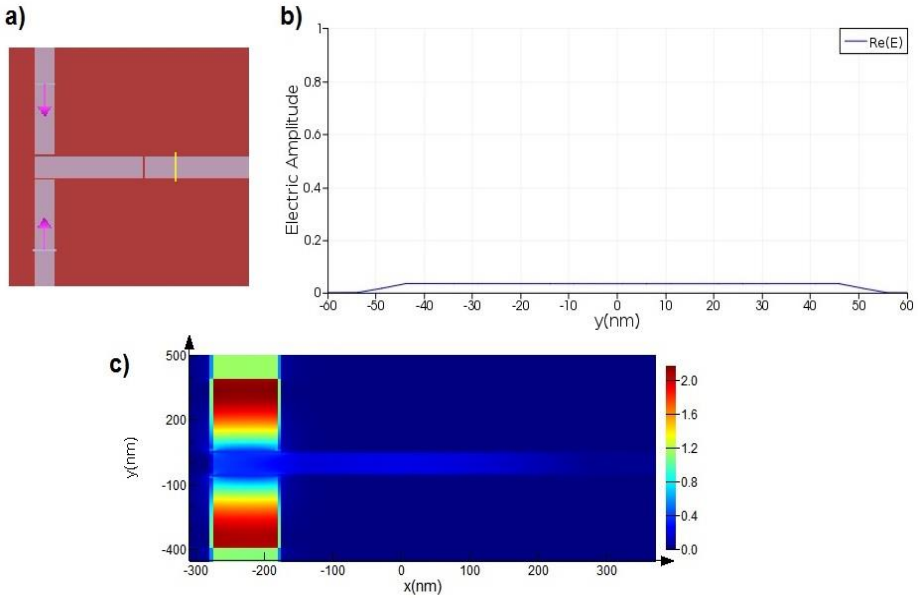

Fig .4. Designed XOR structure a) Stimulation mode of both input ports; b) electric field amplitude at 1550nm at output port; c) display of fields in the gate structure at 1550nm

In Fig. 5a, we stimulate the upper input port with the unit wave amplitude. In this case, the amplitude of the electrical field of the output port is shown in Fig. 5b at 1550nm where the range of the field is 0.62 and greater than the value of the solid state, which is considered as logical 1.This suggests the correct performance of the XOR gate in this mode. In Fig. 5.c, the range of fields is observed in the equipment and the input/output ports.

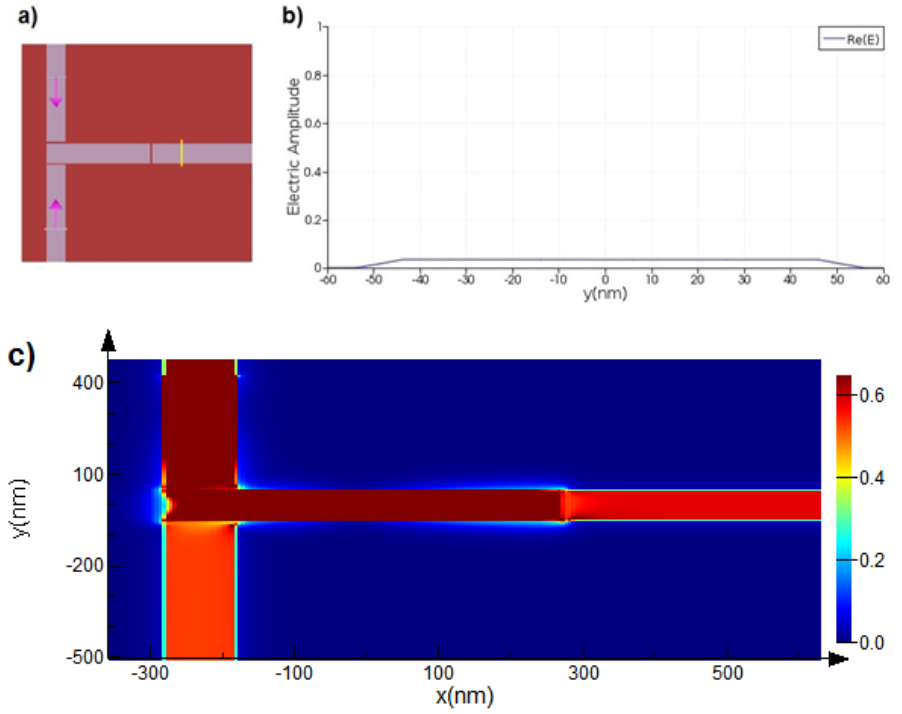

Fig .5. Designed xor structure a) Upper input port in stimulation mode; b) Electrical field amplitude at 1550nm at output port; c) Display of fields in the gate structure at 1550nm

4. AND LOGIC GATE

For the proposed AND gate, as shown in Fig. 4, two input ports are used for bits ‘a’ and ‘b’, while employing one output port ‘c’. When one of these ports has an optical electrical field greater than 0.4, it will be logic ‘1’. The dimensions of nano-resonators are as follows: Ls=580 nm and W=100 nm. For the central wave length, the optimized value will be 1550 nm. The distance between each of the input and output waveguides and the 10-nm resonator for the maximum resonance after optimization sweeps has been considered using FDTD. In Fig. 5a, both inputs are excited by an optical field with an amplitude of 1. Fig. 5b depicts the resonance frequency of the resonator at 1550 nm.

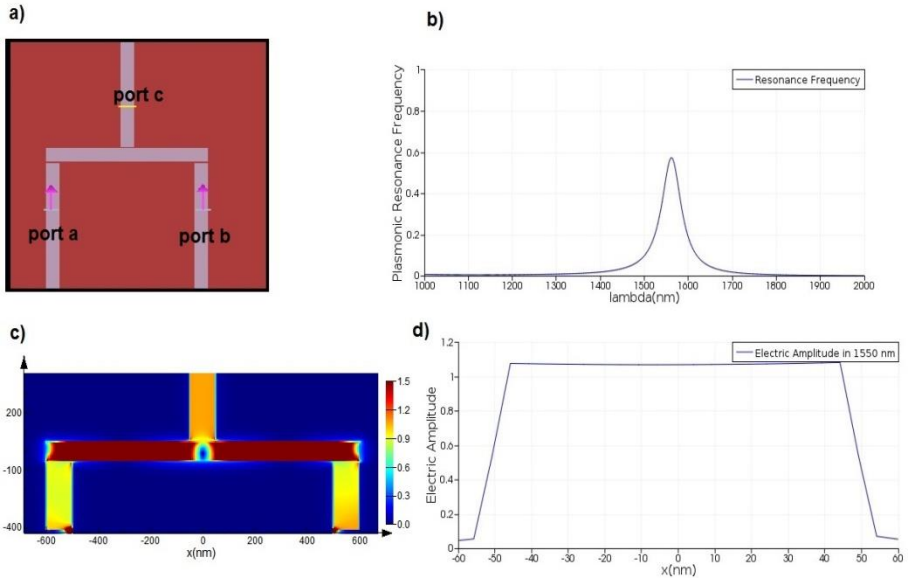

Fig. 6. Designed by the AND gate structure, a) Stimulation mode with both input ports, b) resonant graphs in a rectangular nanosorator, c) display of fields in the gate structure at 1550nm, d) electric field amplitude at 1550nm in structure

Fig. 6c represents the electric field intensity at 1550nm. As can be observed, the field intensity is significant within the nano-resonator, which is up to several times greater than the field amplitude in the input ports, because of frequent resonances and addition of their amplitudes. Fig. 6d demonstrates the optical electric field with amplitude of 1.1. As its value is greater than the conventional 0.4, thus, the output is logic '1'. Also, the true function shows the AND gate in this state.

In another mode, only one of the inputs has been active and the other remained in active i.e., a=1 and b=0. Further, the circuit output is shown in Fig. 7b in which the electric field amplitude is approximately 0.3, which is less than the conventional 0.4, leading to logic '0.'

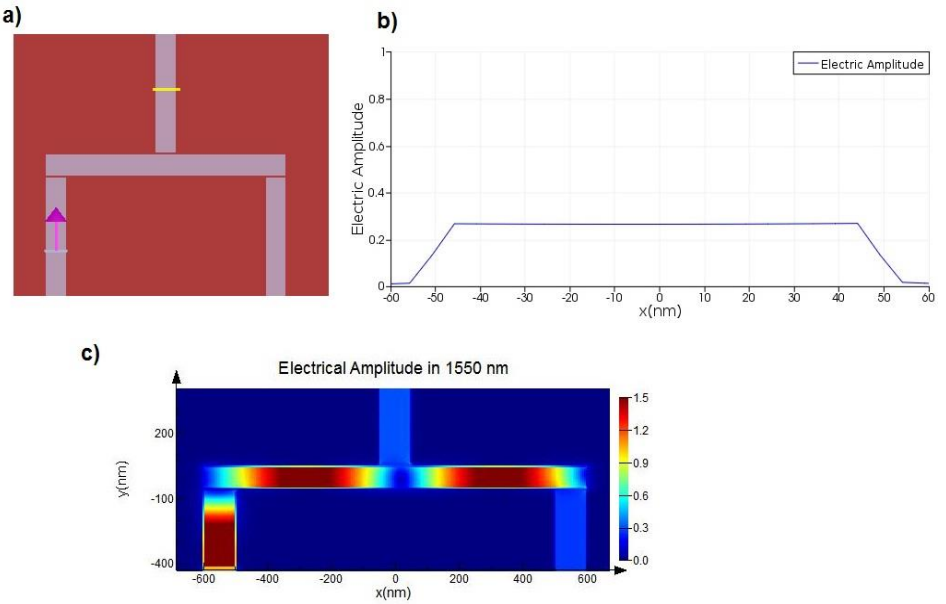

Fig .7. Design of the AND gate structure, a) the stimulation mode with the left input port, b) the electric field amplitude at 1550nm at the output port, c) the display of the fields in the gate structure at 1550nm

Fig. 7c illustrates the electric field amplitude. We observe that although the field amplitude in the nano-resonator is high, the field amplitude in the output port is very small (roughly zero), yielding the expected logic '0'.Due to the circuit symmetry, the third mode (a=0 and b=1) leads to the outputs/results similar to Fig. 5.

5. THE PROPOSED HALF-ADDER CIRCUIT USING A FOREMENTIONED LOGIC GATES

Fig. 7 displays a half-adder consisting of two gates: XOR and AND. Likewise, all dimensions are similar to the case of logic gates except that for establishing settings at the level of output fields, the distance between waveguide C and nanoresonator nanoring has been increased to 15 nm. The rational boundary for this half-adder is E=0.5. This suggests that each port where the electric field amplitude is greater than 0.5 leads to logic '1'; otherwise, logic '0'.

Previously it was assumed that the input ports are a=1 and b=0 (i.e., an optical electric field with an amplitude of '1' is activated in port 'a'). In this case, the structural schema is according to Fig. 5aa. The optical electric field amplitude in the output ports of C and S has been measured at the wavelength of 1550 nm (See Fig. 5c and 5b). Expectedly, the electric field amplitude in port S is 0.62

representing logic ‘1’. On the other hand, the field amplitude in port C is 0.45, which is less than boundary value, indicating logic ‘0’.

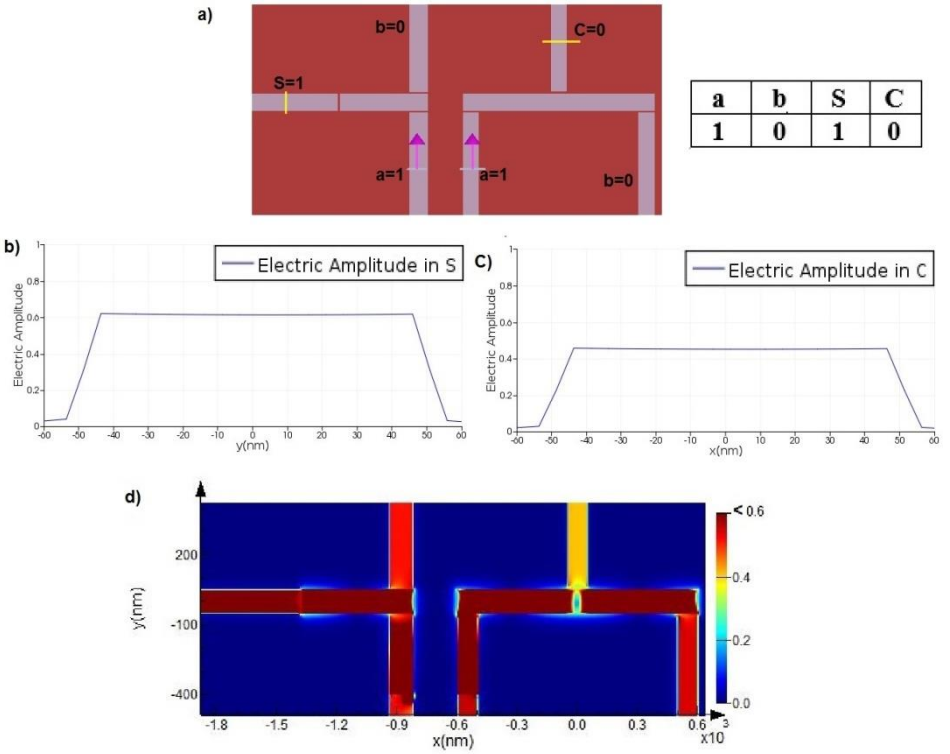

a	b	S	C
1	0	1	0

Fig .8. half-adder structure a) Sum of a = 1, b = 0; b) electric field amplitude diagram at 1550nm at output port S; c) electric field amplitude curve at 1550nm at output port C , d) showing the electric field at a wavelength of 1550 nm in the structure

Due to the symmetry in the circuit for a half-adder, it can be indicated that the second case (a=0, b=1) has also similar results as the first case. Until now, the developed half-adder worked properly and now (in the third mode) both input ports of logic’1’ should be considered.

In the third case, it is assumed that the input ports are a=1 and b=1 (that is, two optical electric fields with an amplitude of ‘1’ are activated in ports 1 and b). In this case, the schema of the structure is revealed in Fig. 6-2, where the amplitude of optical electric field in the output ports C and S has been measured at the wavelength of 1550nm (See Fig. 5-c and Fig. 5-b). Expectedly, the electric field amplitude in port S is less than 0.001, indicating logic ‘0’.On the other hand, the field amplitude in port C is 0.9,which is higher than the boundary value, leading to logic ‘1’.

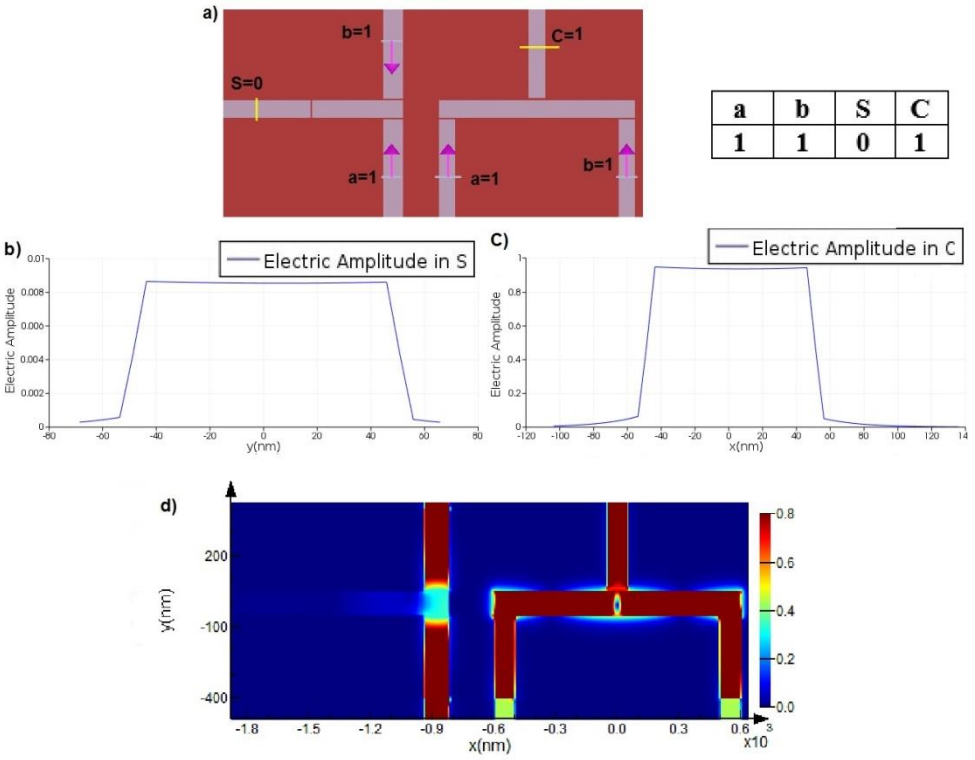

a	b	S	C
1	1	0	1

Fig .9. Half – adder structure a) Sum of a = 1, b = 1, b) Electrical field amplitude diagram at 1550nm at output port S, c) Range of electric field amplitude at 1550nm at output port C , d) showing the electric field at a wavelength of 1550nm in the structure

6. THE PROPOSED FULL-ADDER CIRCUITS

For being applicable to all-optical calculators, the adder circuit proposed in the previous section should add the bit from previous levels to the bits ‘a’ and ‘b’ in order to achieve a full adder. We can see in Fig. 9 that with series connection of two half-adders and OR gate, a full adder can be designed. The logic table of a full adder is given in Fig. 9.

A full adder may be obtained simply via series connection of two previous half-adders (See Fig. 9). However, due to large photo drop in each half-adder, and in turn, photo drop in the OR gate, the output will have low photo power and the amplitude of the photo electric field in the output falls below 20% of the input photo wave amplitude, which is one of the shortcomings of this full-adder circuit. In this paper, a full-adder circuit is obtained with the minimum loss of photo power using a three-input OR gate, two-input AND gate previously designed and three-input XOR gate. They operate based on the following relation:

$$S = A \oplus B \oplus C$$
$$C_{out} = A.B + A.C_{in} + B.C_{in}$$

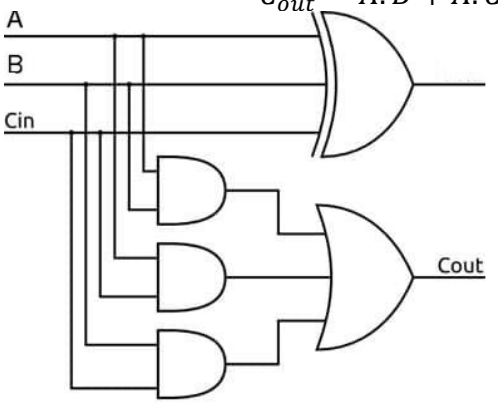

A	B	C_{in}	Sum	C_{out}
0	0	0	0	0
0	0	1	1	0
0	1	0	1	0
0	1	1	0	1
1	0	0	1	0
1	0	1	0	1
1	1	0	0	1
1	1	1	1	1

Fig. 10. Schematic diagram of optical full-adder logic circuit with the correct logic

7. THREE-INPUT OR LOGIC GATE

Fig. 10 demonstrates the structure of the three-input OR gate. The amplitude threshold of the photo electric field in the waveguides is 0.4. When the field amplitude exceeds 0.4, a logic '1' develops; otherwise logic '0' is obtained. In the first mode, all three inputs are assumed to be active. In this case, the output photoelectric field amplitude is approximately 1.5 (as seen in Fig. 10c). As its value is greater than 0.4, expectedly a logic '1' is developed. Fig 10c illustrates the electric fields in the structure of OR gate. As can be observed, the circuit operates properly.

In the second mode, one unexcited input and two photo excited inputs are assumed. Fig 11a reveals the input, while Fig 11 shows the electric field amplitude in the output (which is 1.1). As it is greater than the threshold, a logic '1' is obtained. Fig 11 indicates the electric fields in the structure of OR gate. The circuit operates properly and the waveguide-side of C changed into orange colour due to the field resonance of the rectangular resonator, representing a resonated field within waveguide C.

In the other modes with two excited inputs and one turned-off input, the condition has similar to the previous mode. Thus, they are not expressed to avoid repetition. In the third mode, one of the inputs is excited while the other two inputs are inactive. In this case, Fig. 11 shows the input, where the electric field amplitude is roughly 0.7. As it exceeds the threshold, a logic '1' is obtained, indicating proper operation of the circuits. In this case, due to the field resonance on waveguide-C and -B sides, the rectangular resonator turned yellow. This suggests that the resonated field enters these two waveguides. In the last case, with three turned-off inputs, there is no field logically connected

to the output port, and thus the electric field amplitude in the output port is zero. This indicates proper operation of the proposed three-input OR gate.

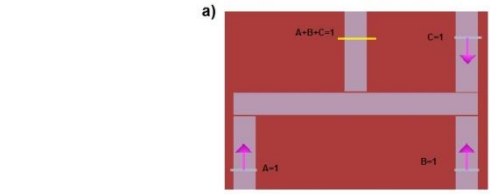

A	B	C	A+B+C
1	1	1	1

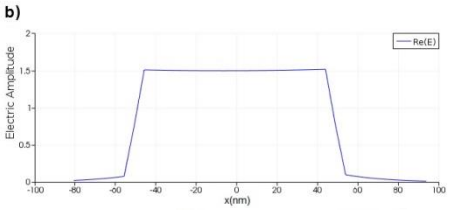

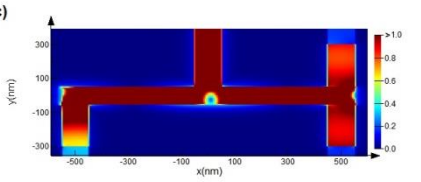

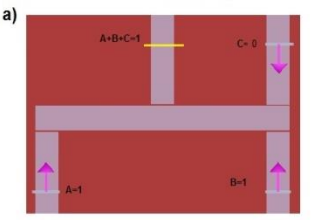

A	B	C	A+B+C
1	1	0	1

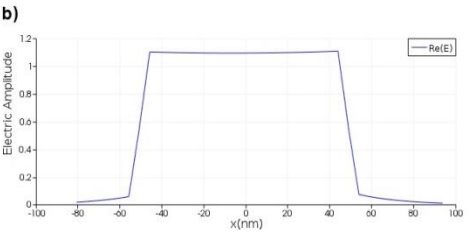

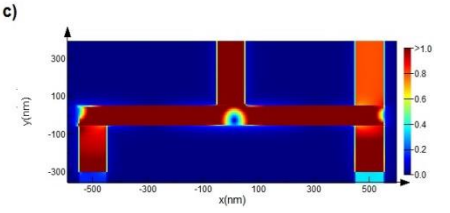

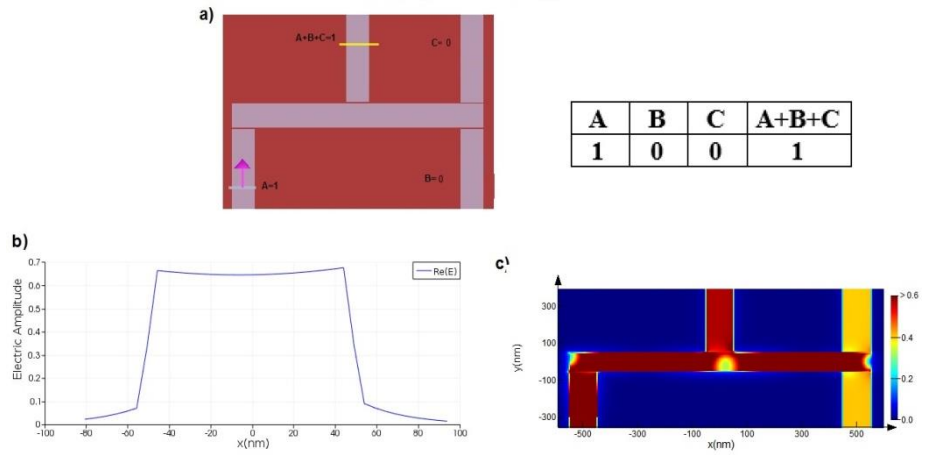

A	B	C	A+B+C
1	0	0	1

Fig. 11.structure OR designed with 3 inputs, a) the stimulation mode of each of the 3 input ports, b) The electric field amplitude at 1550nm at the output port and c) displaying the fields for different input in the gate structure at 1550nm

8. THREE-INPUT XOR LOGIC GATE

In order to design the proposed full adder, a XOR gate with three inputs (Fig. 13) is required. The depth of interest for silver is 50 nm (Drude model has been considered for silver). The width of all waveguides is 100 nm and all distances between waveguides and nanoresonators as well as the distance between two nanoresonators have been optimized at 10 nm. The threshold in this structure is 0.1, suggesting that when the electric field amplitude in the output is greater than 0.1, a logic '1' is obtained. However, when its value is zero or near 0.1, a logic '0' is gained.

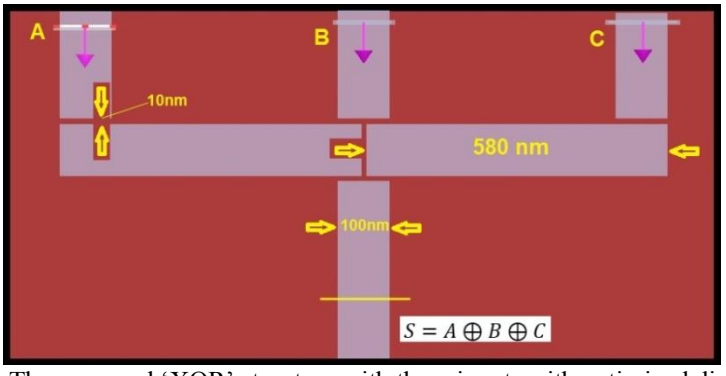

Fig .12. The proposed 'XOR' structure with three inputs with optimized dimension (simulation is done with values: d=10nm, W=100nm, Ls=580nm)

The first case of simulations is related to activation of one of the inputs by an electric field with amplitude of 1 and wavelength of 1550nm. In this case, the output of 'XOR' has a field value according toFig. 12. Also, the waveforms are according to Fig. 13a in the structure of the wavelength of 1550nm.
As can be seen in Fig. 13b, the electric field in the output is greater than 0.4 and, thus, a logic '1' develops. Due to symmetry, if only the input of C is activated, the conditions will be as previously obtained (not mentioned again for the sake of brevity). Now, it is assumed that only the middle input, i.e. B waveguide, is activated (See Fig. 13a). In the next stage, two active inputs and one inactive input are available. First, the case of A=1, B=1, C=0 is considered. In this case, it is expected that the value of XOR becomes zero. Once the simulations are completed, the waveforms of fields are according to Fig. 13c. Two output waveguides observed for the electric field amplitude at the wavelength of 1550nm are approximately zero. This suggests that a logic '0' is obtained. For the other two cases, the conditions are similar due to symmetry of the structure. Thus, they are not included for the sake of brevity.

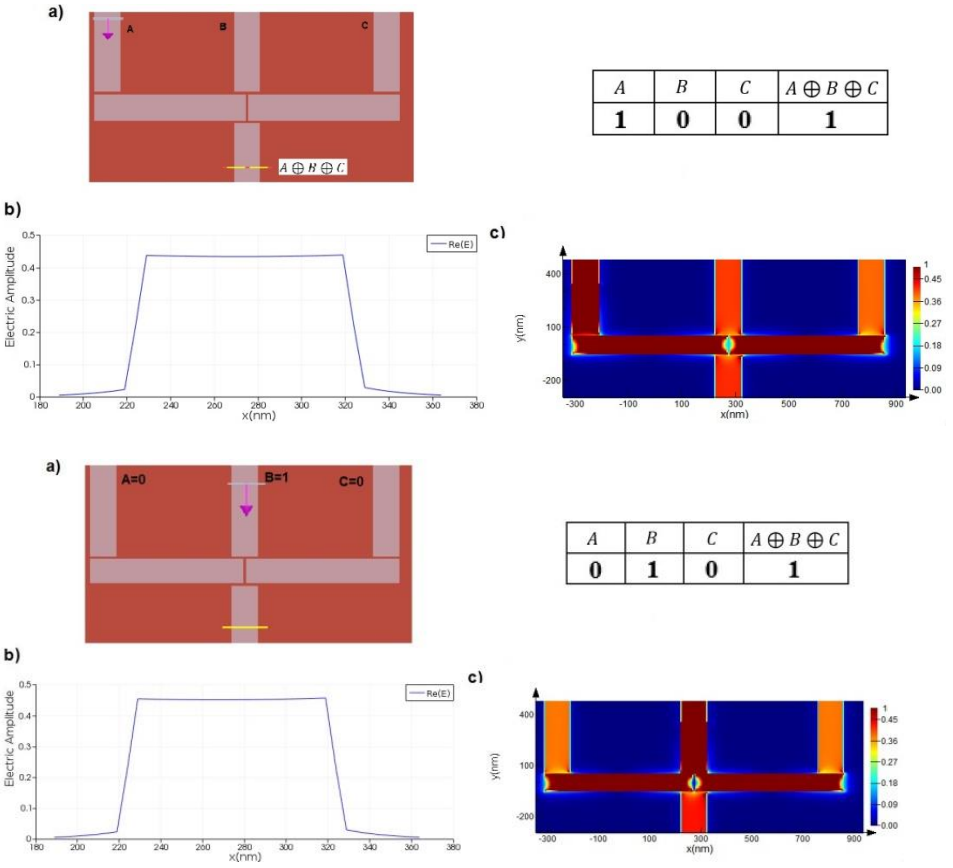

A	B	C	$A \oplus B \oplus C$
1	**0**	**0**	**1**

A	B	C	$A \oplus B \oplus C$
0	**1**	**0**	**1**

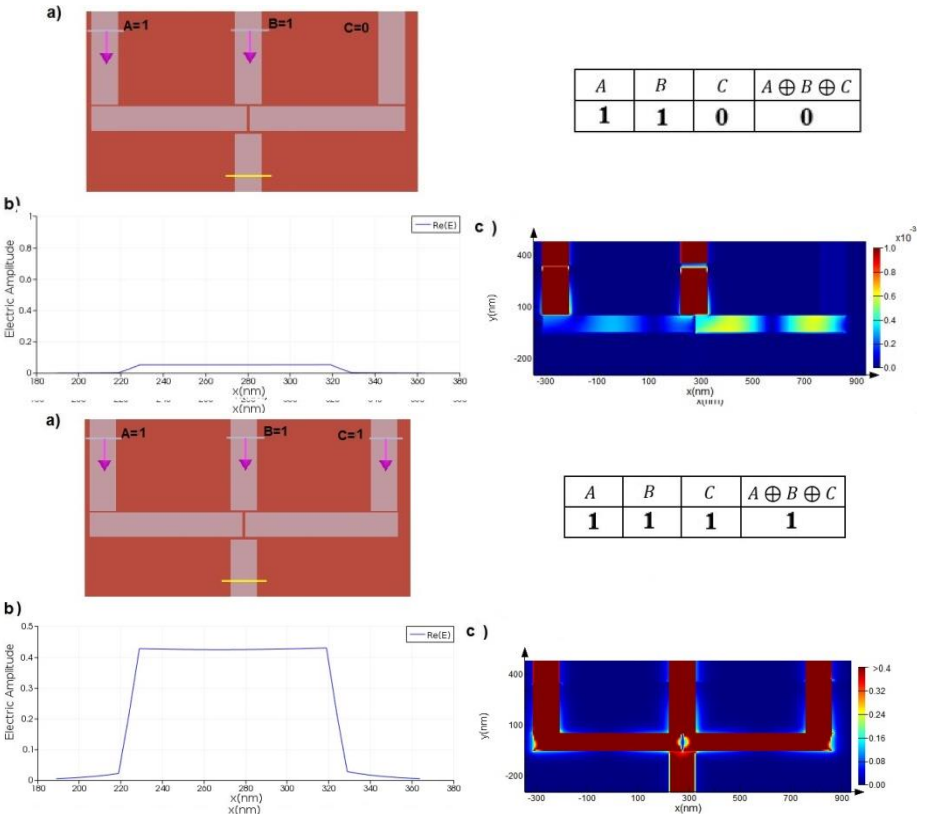

A	B	C	$A \oplus B \oplus C$
1	**1**	**0**	**0**

A	B	C	$A \oplus B \oplus C$
1	**1**	**1**	**1**

Fig .13. XOR structure designed with 3 inputs, a) stimulation mode, b) electric field amplitude at 1550nm at output port, and c) display of fields in the gate structure at wavelength 1550nm for different values of A,B and C (simulation is done with values :d=10nm , W=100nm , Ls=580nm)

In the last case, all inputs are active. Inputs-outputs in this case are according to Fig. 13d and the related logic table is provided in the same Fig. All inputs are excited by a unity electric field amplitude. Its value in the output is greater than 0.4 (as seen in Fig. 13d), indicating a logic '1' and proper operation of the gate in this case. Meanwhile, the waveforms can be observed in Fig. 18c. As can be seen, the field amplitude in the input ports is unity and filled with a red-coloured maximum density. The field amplitude in the output port is 0.4, which is also shown by a red-coloured density.

9. RESULTS and DISCUSSION

The Finite Difference Time Domain (FDTD) is used to simulate the structure and calculate the distribution of electric fields in defective paths. The wavelength chosen for calculations has been 1550 nm. Simulations and calculations have been done for two-and three-input modes. Across all simulations, the constant values for the refractive index (n), length of Ls and coupling distance (d) have been considered fixed. Now, with the increase of the n and Ls of the wavelength value, d also grows which is not desirable. Fig. 19 demonstrates two values of n and Ls. The normalized value of the coupling distance has been 10, which declines with increasing the wavelength. Accordingly, the above discussion only occurs if the gap hole resonator contains one state. In a slot cavity resonator with a length of Ls and refractive index (n), and for a wave with a central wavelength of λ, the wavelength between two neighbouring wavelengths (Δλ) is given by [6,19]:

$$\Delta L = \lambda^2/2nLs$$

Thus, for the central wavelength of 1550nm, in a cavity with a length of 580 nm and filled withn=1, $\Delta L = 2071nm$.The value obtained is greater than the length of Ls, suggesting existence of single mode(Fig. 14)

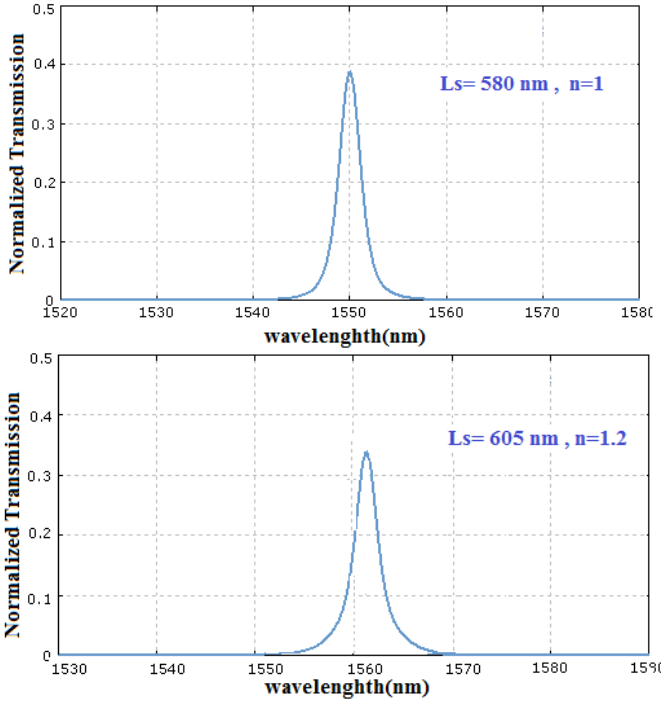

Fig .14. Transmission spectra for different length, Ls and different refractive index, n of materials.

10. CONCLUSION

A full adder circuit was designed considering the designed logic gates by emission f plasmonic waves in the frequency and optical window of 1550 nm with a simple structure. In the second part, for signal transfer, using plasmonic waves a full adder circuit was designed/simulated by OR and XOR logic gates with three inputs and gate 'and.' These gates with three inputs were introduced for the first time in this paper anjoying a simple structure and low cost. In comparison with similar designs in previous research for logic gates using plasmonic waves, the proposed scheme presented a far better performance. Also, the definition of the constraint limit was clearly defined along with the outputs were as logical 0 and 1 plus this one, which is a very important advantage in the design. In the proposed design, by optimizing the dimensions of the structure, we have been able to reduce the losses and achieve a transmission coefficient of 0.62, thereby reducing the losses by 25%.

REFERENCES

[1] S.I .Bozhevolnyi, *Plasmonic Nanoguides and Circuits*, Pan Stanford Publishing Pte. Ltd.(2009)

[2] J .R.Salguiro,Y. S. Kivshar, *Nonlinear plasmonic directional couplers.Appl.* Phys. Lett. **97**, 277-279 (2010)

[3] Y. Fu, X Hu, C. Lu, S Yue, H Yang, and Q Gong, *All-Optical Logic Gates Based on Nanoscale PlasmonicSlot Waveguides*, Nano Lett. **12**(11), 5784–5790 (2012)

[4] A.Kumar, S. Kumar, S.K.Raghuwanshi, *Implementation of fulladder and full-subtractor based on electro-optic effect in Mach–Zehnder interferometer*, Opt. Commun. **324**, 93–107 (2014)

[5] M. Kaboli and M. Akhlaghi, *Investigating the optical AND gate using plasmonic nanospheres*, J. Comput. Electron **15**, 295–300 (2016)

[6] A. Dolatabady, N. Granpayeh, *All-optical logic gates in plasmonic metal–insulator–metalnanowaveguide with slot cavity resonator*, J.Nanophoton. **11**(2), 45-52 (2017)

[7] V. Alwayn, *Optical Network Design and implementation*, Cisco Press, Mar. (2004)

[8] P. B. Johnson and R. W. Christy, *Optical constants of the noble metals*, Phys. Rev. B **6**(12), 4370–4379 (1972)

[9] D. Pan, H.Wei and H. Xu, *Optical interferometric logic gates based on metal slot waveguide network realizing whole fundamental logic operations*, OPTICS EXPRESS 9556, 22 April9556-9562 (2013)

[10] M. Rezvani,M. Fathi Sepahvand, *Simulation of Surface Plasmon Excitation in a Plasmonic Nano-Wire Using Surface Integral Equations*, Journal of Optoelectronic Nanostructures. **1**(1) 54-63 (2016)

[11] A.Kotb, *Simulation of soliton all-optical logic XOR gate with semiconductor optical amplifier*, J. Opt. Quantum Electron. 48 (5) (2016)

[12] K. Goudarzi, A Mir, I. Chaharmahali, D. Goudarzi, *All-optical XOR and OR logic gates based on line and point defects in 2-D photonic crystal*, Optics &Laser Technology, 78, 139-142 (2016)

[13] A. Salmanpour, S. Mohammadnejad, A. Bahrami, *All-optical photonic crystal AND, XOR and OR logic gates using nonlinear Kerr effect and ring resonators*, Journal of Modern Optics, **62** (9), 1-8 (2014)

[14] A. Pashamehr, M. Zavvari, H. Alipour-Banaei, *All-optical AND/OR/NOT logic gates based on photonic crystal ring resonators*, Frontiers of Optoelectronics **9**(4) 578-584 (2016).

[15] M. M. Karkhanehchi, F. Parandin, A. Zahedi, *Design of an all optical half-adder based on 2D photonic crystals*, Photon Netw. Commun., **33**(2) 159-165, (2017).

[16] Y.Zhang, Y. Chen, X. Chen, *Polarization-based all-optical logic controlled-NOT, XOR, and XNOR gates employing electro-optic effect in periodically poled lithium niobate*, Appl. Phys. Lett. **99,** 161117 (2011).

[17] H. Alipour Banaei, H. Seif-Dargahi, *Photonic crystal based 1-bit full-adder optical circuit by using ring resonators in a nonlinear structure*, Photonics and Nanostructures-Fundamentals and Applications, **24,** 29-34 (2017)

[18] M. Mansouri, A. MirNumerical, A.Farmani, *Modeling of a Nanostructure Gas Sensor Based on Plasmonic Effect*, Journal of Optoelectronical Nanostructures, **4**(2) 29-44 (2019)

[19] G. Keiser, *Optical Fiber Communications*, 3rd ed., *McGraw-Hill*, New York City (2000)

[20] S. Serajmohammadi, H. Alipourbanaei, and F Mehdizadeh, *Proposal for realizing an all-optical half adder based on photonic crystals*, Applied Optics,**57**(7) 1617-1621 (2018)